

Lane determination with GPS Precise Point Positioning

Victor L. Knoop, Peter F. de Bakker, Christian C. J. M. Tiberius, and Bart van Arem, *Senior member, IEEE*

Abstract—Modern Intelligent Transport Solutions can achieve improvement of traffic flow on motorways. With lane-specific measurements and lane-specific control more measures are possible. Single Frequency Precise Point Positioning (PPP) is a newly developed and affordable technique to achieve an improved position accuracy compared to Global Positioning System (GPS) standalone positioning. GPS-PPP allows for sub-meter accurate positioning, in real time, of vehicles on a motorway.

This paper tests this technique in real life; moreover, it presents a methodology to map the lanes on a motorway using data collected by this technique. The methodology exploits the high accuracy and the fact that most driving is within a lane. In a field test, a GPS-PPP equipped vehicle drives a specific motorway stretch 100 times, for which the GPS-PPP trajectory data are collected. Using these data the positions and the widths of different lanes are successfully estimated. Comparison with the ground truth shows a dm accuracy. With the parametrized lanes, vehicles can be tracked down to a lane with the GPS-PPP device.

I. INTRODUCTION

Intelligent Transport Solutions generally work by measuring traffic and applying control measures. Traditionally, measuring and informing traffic takes place through road-based systems, but this is changing now towards more in-vehicle systems. One of the requirements for more advanced motorway traffic control is that lane-specific measurements can be made, and vehicles can be provided with a lane-specific control measure. For in-car systems it is hence required that the position is known with an accuracy better than the width of a lane. Several techniques are known, for instance using differential GPS (D-GPS) [1], or with the aid of vision [2] or radar [3] to improve a rough map.

This paper tests a new technique that improves the accuracy of the position based on signals from the Global Positioning System (GPS). This technique does not need expensive equipment and does not rely on vision or radar, hence works in all weather and light conditions. This technique is able to determine the position of a car more accurately than the width of a lane. However, in most digital maps separate lanes are not yet indicated. Therefore, a main contribution in this paper is the technique, as well as a methodology to find the lanes automatically based on trajectories collecting using the GPS technique. We have previously already presented some of our techniques [4], [5] and measurements [6]. For completeness of the current paper, slightly modified versions of relevant paragraphs of these respective papers are again included here.

Hence there is overlap with these papers, especially with (an earlier version of) the content presented at the 16th International IEEE Conference on Intelligent Transportation Systems (ITSC2013) and published with the digital object identifier 10.1109/ITSC.2013.67284563, [6]. Content-wise, the current article combines and further develops the above-mentioned three works. Notably, the lanes are found in a better, more robust way. Moreover, the end results in terms of lane positioning are now compared to the locations of the lane markings in the official database of the road authority, whereas in earlier publications only the internal consistency of the lane locations was considered.

The structure of the paper is in line with the steps of the research. First, in the next section, we review various vehicle positioning techniques, next we present the main ideas of the GPS-PPP technique. Then, section IV discusses the experiments. Section V then shows how the lanes are found, and the results of that process with the experimental data. A more robust way to find lanes, combining different base points into clustered points, is presented in section VI. Section VII shows how the results change if the lane width has to be estimated as well. In all cases, the results of the lane positions are presented on a map which also shows the accurately surveyed location of the road markings as provided by the road authority, called the digital topographical file. Finally, section VIII presents the conclusions.

II. MONITORING THE POSITION OF A VEHICLE

The position of a vehicle can be monitored by various sensors. This section discusses which types of sensors and techniques can be used to obtain the vehicle position. First, the GPS techniques are described followed by a part on techniques using vision.

An overview of the GPS techniques is given in [7]. For mapping the vehicle position to the road, sophisticated algorithms have been developed (e.g., [8], or [9] with incomplete data). The usual problem in GPS positioning is that the accuracy is not within a lane-width, hence lane-mapping or mapping the position to a *lane* is impossible. In (urban) canyons, the accuracy decreases since there is no line of sight to some satellites, requiring further approximations (e.g., [10]). Anyway, solutions have to be found to improve the accuracy to get accuracy to a lane level. For instance D-GPS is being used, e.g. by [11] and [12].

[13] discuss the option of creating lane-specific maps, in a dedicated mapping campaign, by using high-end dual-frequency GPS receivers in a differential (carrier-wave) processing setup. They discuss problems with driver errors and

difficulties finding the lane boundary demarcations with this approach. They propose an alternative method that uses geo-corrected aerial photographs and manual lane finding. Our solution, on the other hand, does not require any manual labour, special equipment or dedicated mapping campaigns, and thanks to the large number of GPS traces, driver errors can be expected to even out. Further fusion with other data from video is proposed by [14]. Also further combination with more epochs of GPS measurements is possible, using Kalman filtering to combine inputs [15]. In these cases, the accuracy of the location improves.

Another way to get an accuracy of positioning down to the lane level, is vision: using cameras which detect the lane markings. [16] provides an overview of the state-of-the art of the techniques in 2014, but it has to be said that the field of image analysis is rapidly developing. Traditionally, this is being used as positioning of the vehicle within the lane (lane keeping) and not as a way to find the lane a vehicle is driving in. The main difference between the two is that in the former case, only markings for the lane the vehicle is driving in have to be found, whereas for the latter case, *all* lane markings have to be found. In all cases, clever algorithms for image processing are needed to detect lanes and analyse the video (e.g., [17], [18]). Without interpretation, vision is not sufficient for finding all lane markings [19]. To improve the detection and speeding up the real-time detection [20] propose to first reduce the dimensionality of the video by making the appropriate transformations; these techniques are also targeted to make automated driving possible. In all cases, vision depends on the quality of video, and hence bad weather and or darkness can hamper the results. Besides, the vehicle position within the lane is known, but this information cannot be used to create a digital map including the positions of the lanes.

This might be further improved by fusing vision data with GPS data (e.g., [21]), or combining the GPS with other features which are measured by the car [22], [23].

The method to create this map and to measure a vehicle's position down to the accuracy of lane using a low-cost sensor is lacking. This paper introduces this method, providing both the positioning techniques as well as the algorithms used to map the lanes.

III. GPS SINGLE FREQUENCY PRECISE POINT POSITIONING

The Global Positioning System has become ubiquitous for personal and automotive navigation after reaching its full operational capability in 1994. The positioning accuracy is sufficient for car navigation under most circumstances (especially since 2000 when the intentional degradation of the signal for non-military use was ceased), and, unlike dead reckoning systems using distance and heading measurements to compute the position, the error in GPS positions does not accumulate over time. Furthermore, the cost of simple GPS receivers has decreased dramatically over time and is no longer prohibitive for mass market applications.

Several different positioning strategies based on Global Navigation Satellite System (GNSS) measurements exist. The

most basic positioning technique is stand-alone GPS positioning in which pseudo range measurements (derived from the observed travel times of the signals) to at least four satellites are used to solve for the three receiver coordinates and its clock offset, while keeping the satellite positions and clock offsets fixed to the predicted values computed by the GPS ground segment. Typically, there is an error of several meters in these predicted trajectories, leading to a similar error in the position estimate for the user. Another source of errors in GPS measurements is the disturbance of the signal in the atmosphere, in particular in the troposphere and ionosphere, leading to errors in the order of several meters to several dozens of meters. Troposphere delays can be mitigated with an a-priori model, and, for high accuracy applications, by estimating a residual effect from the measurements. Ionospheric delays in the signal cause errors. A-priori ionosphere models are only effective in removing about half of the effect, leaving a positioning accuracy in the order of several to tens of meters. Alternatively, one can estimate the delays by collecting data on two frequencies, at the expense of a high-end GPS receiver. Regional Satellite Based Augmentation Systems (SBAS) can improve the accuracy to a few meters by computing more accurate satellite positions, clock offsets and modeling the regional ionospheric delays.

Even much higher accuracies can be reached by computing (relative) positions with respect to a nearby reference station for which accurate coordinates are available, because of the strong spatial correlation of a number of error sources including the ionosphere delays, which are consequently largely eliminated in differential positioning. Other than the pseudo range measurements, the much more precise carrier phase measurements can also be used in differential positioning, provided the unknown carrier phase cycle ambiguities can be solved to their integer values. In this case the position accuracy can reach cm or even mm level. However, the disadvantages of differential positioning are (1) it relies on a dense local/regional network of reference stations and (2) needs large data transfers (typically a correction for each signal at each epoch) between the reference stations and each user, thereby making it unsuited for mass market applications.

GPS Precise Point Positioning (PPP) also uses both pseudo range and carrier phase measurements, [24]. However, contrary to differential GPS, it combines them with accurate satellite orbit and clock information (from a relatively sparse global tracking network) instead of measurements from a nearby reference receiver. Thereby the PPP approach negates both aforementioned disadvantages while keeping the accuracy high. [25] report decimeter-level positioning accuracy for 20-30 minutes of continuous kinematic observations, and even better performance for static observations. Traditionally, PPP has several limitations:

- 1) Accurate satellite orbit and clock information was initially only available with significant delays, restricting PPP to post processing applications.
- 2) Dual frequency measurements were needed to eliminate the ionosphere delays from the measurements, demanding relatively expensive user hardware.
- 3) The necessity to eliminate the ionosphere, and to es-

time the carrier phase ambiguities at the same time, gives a relatively weak model and consequently leads to significant delays – the so-called initialization time – before the positioning solution converges to a sufficiently high accuracy.

Over the last decade much effort has been spent to overcome these disadvantages. Nowadays, accurate (predicted) satellite orbits are available in real-time together with (near) real-time satellite clock estimates, overcoming the first limitation [26], [27]

The use of a single-frequency receiver would significantly reduce the cost of PPP, but requires a different approach to negate the ionosphere delays. One approach, known as GRAPHIC (Group And Phase Ionospheric Correction) [28] is to average the pseudorange and carrier phase measurements for each satellite. Since the first order ionosphere delay has the same magnitude but opposite sign on the pseudorange and carrier phase measurements, it is eliminated if the average is taken. The resulting single-frequency ionosphere-free observation has about half the pseudorange measurement noise. However, it also contains the carrier phase ambiguities, which actually makes problem 3 above worse. Chen et al. [29] who use GRAHPIC for lane detection, indeed report that 30-60 minutes are required for the convergence of the estimated ambiguities at initialization. A similar period might be expected after temporary loss of signal reception.

At Delft University of Technology, an alternative Single Frequency (SF) PPP algorithm has been developed that uses (predicted) ionosphere maps instead of estimating the ionosphere delay from the observations. As a result, the position accuracy improves much faster than that of traditional dual frequency PPP and the GRAPHIC method, reaching an accuracy of several decimeters already within a few epochs (i.e. seconds) [30].

Since this new technique can be implemented on a relatively cheap GPS receiver for the user (as only single frequency measurements are needed) and it provides a highly accurate position, it opens a wide range of applications in different fields including automotive and hand held GPS devices. A specific application is the use for lane identification, for which it was already demonstrated to meet the accuracy requirement; a successful automotive experiment was presented at the ION GNSS 2011 conference [4].

Precise Point Positioning is favored for many applications, thanks to its very high accuracy and independence of a local infrastructure, examples are crustal deformation monitoring, precision farming, to support seafloor mapping, and land surveying [25]. However, due to the long (convergence) time to reach a high accuracy, conventional PPP is best suited to static applications, or other applications where uninterrupted satellite tracking is possible.

Our suggested approach on the other hand, is to use single-frequency PPP, which shares the independence of local infrastructure, but does not reach the same level of accuracy, which makes it less interesting for most conventional PPP applications. However, thanks to the low cost hardware, and short convergence time, it is perfect for dynamic applications with quickly changing sky-view, and where many receivers may

be needed with competitive accuracy and price, or simply where dual-frequency PPP is too expensive. Examples are hand-held devices, buoys, low-cost precision farming, and automotive applications.

For the experiments described below, the solution has been calculated afterwards, but only using data which was available at the time of the observation (hence replaying a real-time scenario). The required bandwidth to get the information in the vehicle is approximately 3 kbit/s – most of which is used to communicate corrections for the satellite positions and clocks (now estimated and relayed at a frequency of once every 5 seconds). This falls well within the bandwidth currently available with 2.5/3G networks. Note that the frequency of measuring the user position is independent of this frequency of updating the corrections to the satellite positions and clocks, and can be much higher (10 Hz in our experiment).

IV. EXPERIMENTAL SETUP

In the experiments for this research we drove the same stretch multiple times, thereby creating a distribution of positions. In earlier work we determined that at least 100 passings are required for a single stretch of road to determine the position of the lanes [5]. That is the number of laps we drive in the current experiment to validate our earlier simulation.

In order to collect the necessary GPS measurements, a vehicle was equipped with a single frequency receiver (costing in the order \$100 and representative of an automotive type of GPS chip today) connected to a patch antenna (costing about \$20), see figure 2 and 3. During a period of approximately two weeks in November 2012 a test vehicle was driven the required number of laps on the A13 motorway between exits number 10 (Delft-Zuid) and 11 (Berkel en Rodenrijs), see figure 1. For this road stretch, also the position of the lane separations is known accurately, since this has been recorded by the Dutch road authority (“Digital topographical files”, or DTF). This DTF contains the locations of the road markings at a 5cm accuracy level. Different time frames were selected during the day, considering the ionosphere and traffic activity as well as the number of visible satellites in the sky. Each lap consists of two parts of approximately 5 km of three lane motorway, and two parts of the underlying road network (intersections, roundabout), which we did not consider in this study. Drivers were instructed to drive as they normally would, which were with speeds of approximately the speed limit (100 km/h). In the northbound direction, they were instructed to use mostly the two right lanes, whereas in the southbound direction the left lane was also allowed as they normally would. The combination of the speed and the “keep right unless overtaking” rule means that also in the southbound direction the left lane was also used less than the other two lanes. The roadway is fairly flat and there are no high rise buildings along the road, which might disturb the signal. Generally, these conditions are fairly favourable for GPS positioning. However, the conditions are still considered operational as many overhead signs, street lights, trees and other traffic may cause temporary signal losses and reflected signals.

The collected 10 Hz raw GPS pseudorange and carrier phase measurements were combined with precise predicted satellite

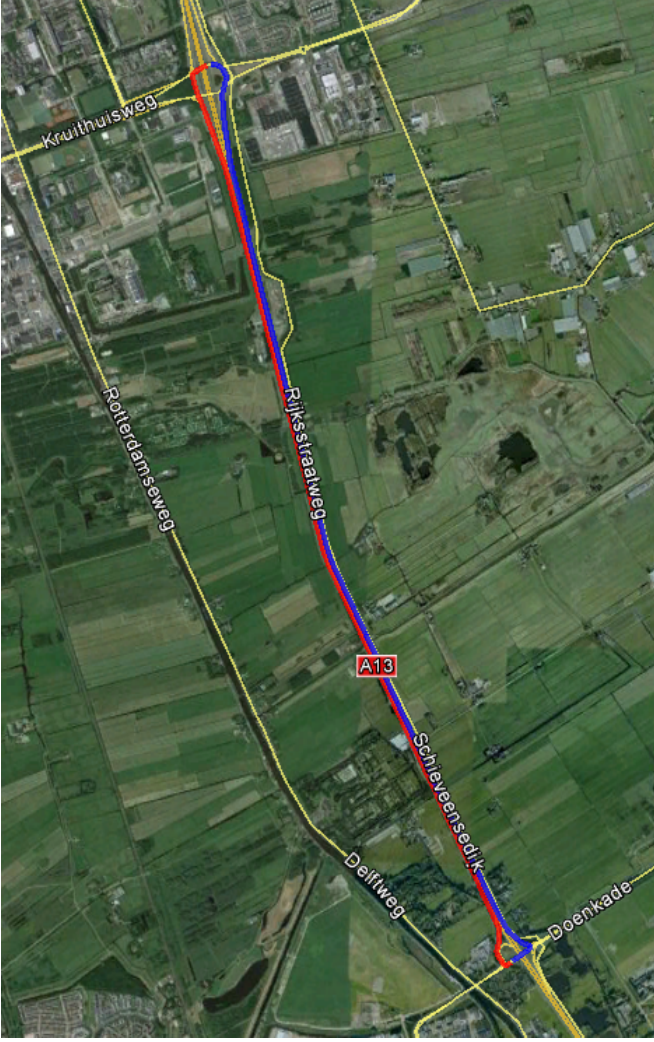


Fig. 1. The test was performed on a 5km stretch of the A13 motorway between Delft (North) and Rotterdam (South), in the Netherlands (figure from Google Earth). The Southbound tracks are indicated with a red line; Northbound tracks with a blue line.



Fig. 2. The u-blox TIM LP single frequency receiver evaluation kit (left) and Tri-M Big Brother patch antenna (right) that were used during the car tests. This hardware is representative of mass-market GNSS hardware for automotive applications.



Fig. 3. The equipment mounted on the vehicle

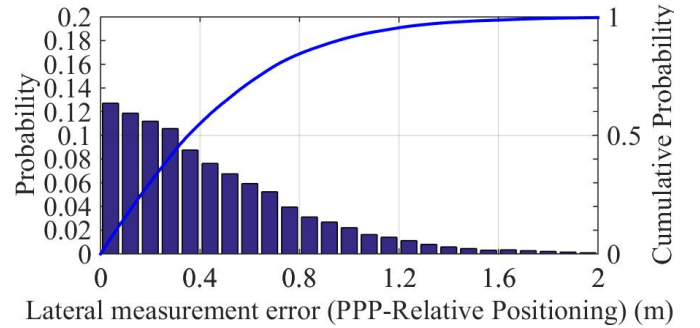


Fig. 4. The histogram and the cumulative distribution of the errors in the GPS-PPP position lateral to the driving direction. The errors are constructed with a cm-accurate differential-GPS position solution as ground truth.

orbits from the International GNSS Service [31], real-time satellite clock offsets from the Real-Time Clock Estimation (RETICLE) system from the German Space Operations Center (GSOC) / German Aerospace Center (DLR) [26] and predicted ionosphere maps from the Center for Orbit Determination in Europe (CODE) [32] (and corresponding satellite differential code biases, DCBs), and processed with our Single Frequency PPP (SF-PPP) algorithms [4]. Troposphere delays were corrected using the (a-priori) Saastamoinen model (accurate to decimeter level in local zenith direction) and a 5 degrees satellite elevation cut-off angle was used [33]. The non-linear SF-PPP model is linearized around an approximate positioning, and the unknown parameters are then estimated with a recursive least squares algorithm.

The estimated unknown parameters consist of the receiver position and clock offset (both estimated each epoch without using a dynamic model) and the carrier phase ambiguities which are kept constant (but not fixed to integer values) if no cycle-slips occur. For a single measurement update this means that the observables are the pseudorange and the carrier phase measurements from the current epoch, and the ambiguity estimates from the previous epoch.

Figure 5 shows the absolute lateral position errors as a function of the number of available satellites by means of

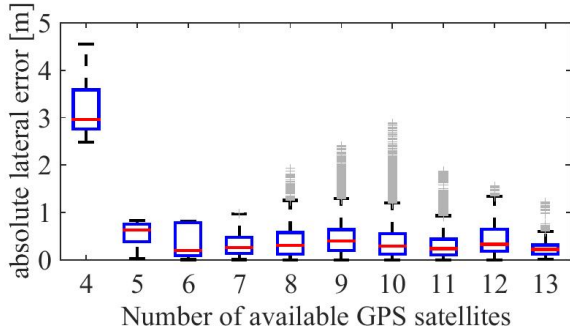


Fig. 5. Boxplot of the lateral position error vs. the number of available GPS satellites (red lines indicate the median value, the boxes indicate 25-75%, and outliers are displayed as gray plus-signs). The position error is sufficiently small for lane identification, if at least 5 satellites are available. Comparison to figure 6 reveals that the number of outliers is directly related to the number of samples in each bin.

a boxplot. For each box, the red line shows the median error for that number of satellites, the edges of the box show the 25th and 75th percentiles, the whiskers extend to the most extreme data points not considered outliers, and outliers are plotted individually in light gray. As is well known for GPS positioning in general, a minimum of 4 satellites are needed to solve the 3 unknown coordinates and the unknown clock offset of the receiver. A minimum of 5 satellites is needed to have some redundancy, and as is clear from figure 5, 5 is also the minimum number of satellites needed to compute an accurate position (with only 4 satellites in view a horizontal position error of 3 to 4 meters can be observed). Considering the boxes for 5 or more satellites, it can be observed that the 75th percentile is somewhat higher for 5 and 6 satellites; for 7 or more available satellites, the 75th percentile is well below the 1 m level. Figure 5 also shows that most outliers are observed for 9 or 10 satellites. However, this is easily explained if we consider figure 6, which shows a histogram of the available number of GPS satellites for each measurement epoch. This reveals a clear relation between the number of epochs and the number of outliers in each bin. The total number of epochs of $6.0e5$ is equal to the measurement duration (approximately 16.7 hours) divided by the measurement interval of 0.1s. Epochs for which no position solution could be computed have been added to the left-most column (<4 satellites). The axis on the right-hand side shows the percentage of the total number of epochs. The figure reveals that 8 to 12 satellites were tracked for most epochs. For 99.21% of the epochs at least 5 satellites were available, enabling accurate positioning for these epochs.

Two high-end receivers were also installed on the car to determine an accurate ground truth for this experiment. For 54 laps, the data from both high end reference receivers were processed with NetPos [34]. Netpos features a network of 35 permanent GPS reference stations across the Netherlands (inter-distances on average about 40 kilometers), and a relative (differential) position solution is obtained for the moving receiver on the vehicle with respect to the network (in fact similar to the classical baseline set-up, with a GPS reference station at a few kilometer distance from the vehicle; though with the network processing more advanced error modeling is

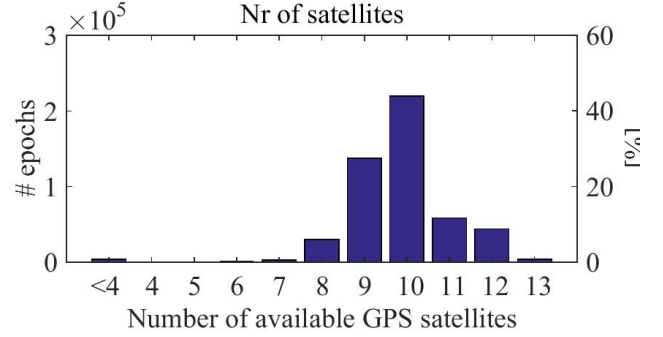


Fig. 6. Histogram of the available number of GPS satellites for all measurement epochs (also as a percentage of total number of epochs). Most of the time, 9 or 10 satellites are available.

involved).

The dominant error sources in SF PPP are the pseudo range measurement noise, multipath delays (caused by reflected signals), residual errors in the ionosphere model, and residual errors in the satellite orbit and clock products. The estimated ground truth is far less sensitive to these errors since the high-end equipment reduces the measurement noise and impact of reflected signals, and the relative set-up largely reduces the impact of ionosphere delays as well as satellite orbit and clock errors. Furthermore, in relative set-up, the accurate carrier phase measurements dominate the positioning (since the integer carrier phase ambiguities can be fixed) reducing the effects of pseudo range measurement errors and multipath delays [35], [36].

Therefore, the ground truth positions have a much higher (cm-level) accuracy than the SF-PPP positions and can be used to assess the errors in the latter. Figure 4 shows the results of this assessment by means of the cumulative distribution of the horizontal errors lateral to the driving direction (relevant for lane positioning and identification). The figure shows that this error was smaller than 0.71 meter for 80%, and smaller than 1.2 meters for 95% of the measurement epochs for SF-PPP. Under comparable conditions, these numbers are respectively 1.44 and 2.27 meters for standalone GPS, a factor two higher which makes it insufficient for lane mapping. These accuracies are in line with the expected accuracy from our SF-PPP solution [4]

V. LANE FINDING ALGORITHM

This section shows a methodology to create a map of the road with all lanes in practice using the GPS-PPP trajectories. This adaptive system map is created just from the tracks of the first group of vehicles driving the road. In this way, the PPP measurement points can lead to a map where other trajectories can be mapped upon. To obtain the digital map with identified lanes, several steps have to be taken. These steps are shown graphically in figure 7. First, GPS-PPP trajectory data in tracks have to be collected. Then, we need to have a reference road to which we relate the track of an individual lap and calculate the lateral offset. The distribution of the offset indicates the location of the lanes compared to the position of the reference

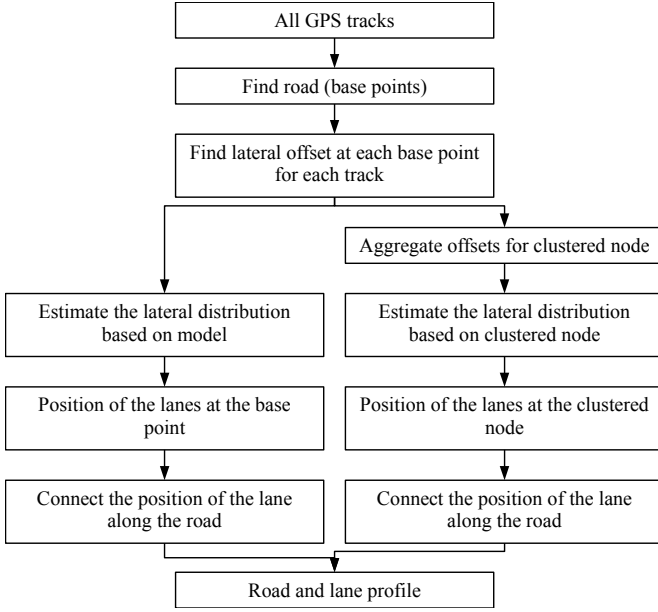


Fig. 7. An overview of the steps taken in the research. In the left branch, the position of the lane is based on measurements for each base point. In the right branch, the lateral passing positions are first combined into clustered nodes for an increased accuracy, and on this larger sample the lane positions are estimated (see section VI).

road. Note therefore that the location of the reference road is not very important.

The reference road is defined by a set of *base points*. In this case, we use the positions of a single run as a basis; for our paper, we choose the first run. The base points on the motorway are approximately 25 meters from each other, which is a good basis for constructing the points at a motorway. The positions of the vehicle are indicated by an east and north component as functions of time $\{E(t), N(t)\}$. On this position, on both the east as well as the north component, a spline is fitted, which removes the noise from the single run. Still, this shows not necessarily the center of the road, but this is not needed for the base points. Lane positions will namely be defined as lateral offset to these base points. The remainder of this section first describes the methodology of finding the lanes, and then presents the results. For the selected stretch of road, the digital topographical files with high accuracy lane positions are available. In the results, the lanes as determined with our proposed methodology as well as the surveyed lanes are shown.

A. Methodology: fitting lanes at base points

For all base points, the positions of the lanes lateral to the roadway are determined. We first have to find the lateral position of the tracks crossing a line orthogonal to the roadway; this is described in section V-A1. Afterwards, the methodology to find the lanes based on these base points is described.

1) *Lateral crossing*: The optimization procedure requires that the lateral positions of the vehicle at a cross section are known. To obtain these for a particular base point i , the following steps are taken (see also figure 8)

- 1) Connect the base points $i - 3$ and $i + 3$.

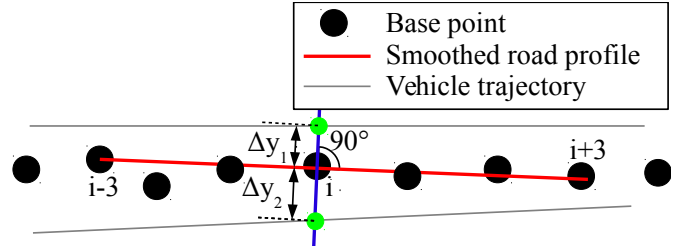


Fig. 8. The lateral positions are calculated by reconstructing where each of the trajectories crosses a line orthogonal to the (average) road direction

- 2) Determine the direction of the road segment, taken linearly between these two points.
- 3) Construct a line orthogonal to the direction of the road, through the base points.
- 4) Determine where each of the GPS tracks crosses this orthogonal line; this gives a set of lateral offsets (Δy) for each of the trajectories. The offsets are indexed for road point i and vehicle v : $\Delta y_{i,v}$

By taking not the direct neighbouring points, but the third point before and after, the road direction is “averaged”. This gives a more robust direction.

2) *Optimization of distribution*: From the lateral crossing points obtained by the methodology described above we estimate the positions of the lanes. Note that a-priori the number of lanes is unknown. We hence estimate the lane positions for roads assuming different numbers of lanes, and then select the best fitting result.

The first step is to make a histogram of the values Δy . The points are distributed in b bins of equal width, in which b is the (rounded) square root of the number of observations. We take the square root of this number as trade-off between the number of bins and the number of observations per bin, which both are preferably high.

Then, the weight in this histogram is compared with a reference function.

$$p(y) = \sum_{l=1}^L \phi_l N(z - lw, \sigma) \quad (1)$$

In this equation, y is the lateral position, l the lane number, L the number of lanes, ϕ_l the fraction of the flow in lane l , $N(X, \mu)$ the normal probability distribution function with mean X and standard deviation μ . z is the offset of the first lane compared to the base path, w is the width of a lane, and σ the width of the distribution of vehicles within a path. This function has the parameter σ , the offset of the first lane, and the lane flow distribution, which adds $L - 1$ parameters (the lane flow distribution adds up to one). This function gives the probability of finding a vehicle at a certain lateral position as product of the probability of finding it in a lane times the a hypothesised normal distribution function for the lateral position of the vehicles within that lane, summed over all lanes. The mid points of distributions per lane are one lane width apart from each other; this lane width is either fixed (section V-B and VI) or found in the optimization (section VII).

The error is found by the differences between the measured relative number of observations (histogram) and the predicted number of observations (reference function) in each bin β .

$$E_\beta = \frac{n(\beta)}{\sum_{\beta \in \text{bins}} n(\beta)} - p(y_\beta) \quad (2)$$

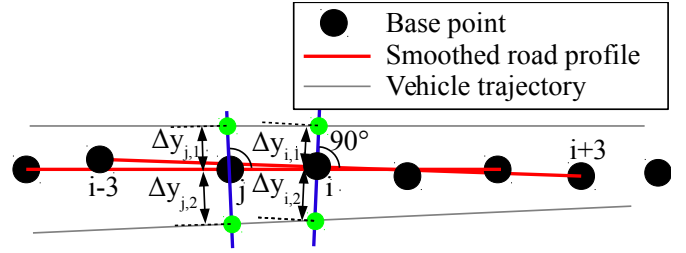
In this equation, y_β is the y-value of the middle of bin β . The goodness of fit is the root mean square of errors E_β . Now, the parameters in the reference function (z, σ, ϕ_l) are adapted such that this error is minimized. This optimization gives the lateral position of each of the lanes for each of the base points. The points for the same lanes can be connected from base point to base point to construct the lateral road profile.

This methodology is similar to [5], but we optimize on the differences in the histogram of the lateral positions, rather than minimizing the KolmogorovSmirnov-distance. In practice, it turned out that the methodology presented here is more robust. It should be noted that the optimization sometimes was aiming at a local optimum where the offset was one lane width more (or less) than on the actual road. For most cases, this problem was solved by optimizing with different initial values for the offset and choosing the one with the best fit, all as part of the automated optimization procedure. If a lane does not contain traffic, it will not influence the distribution of traffic over the lanes, e.g. in the extreme case no vehicle uses the third lane, a fit of a three lane road with an extra unused lane at the left is equally good as the one with the correctly located third one unused. In order to overcome problems with lanes with a fraction of vehicles, we restricted the optimization such that most observations are in the right lane and that each lane obtains at least 10% of the observations. This is true for most observations in the middle of the observed stretch. The second assumption is violated near the entry and exit, and at some locations in the northbound direction.

B. Results

Figure 9(a) shows the histogram of the lateral offset and the fit through the points. As figure 9(b) shows, the estimated road path follows the measured trajectories quite accurately. The lane separations as estimated by our method are very well in line with the digital topographical file; the error is in the order of 2 dm. The error in the northbound direction is slightly higher (error of typically 3 dm), which is most likely due to the low fraction of observations in the left lane. Therefore, the fitting procedure is not able to match the three-lane distribution well.

It should be noted that the fitting procedure is not robust and for several base points no optimal solution is found. This has mainly to do with the optimization method and the constraints. The error which occurs most frequently is that the estimation is off by one lane. This is due to the initial value and the constraints on the amount of vehicles in one lane, which does not always match the location of the base point or the lane flow distribution. For the current purpose, optimization procedure (with different initial points) works well. An additional check on the road jumping by one lane for one point and back the next point – indicating an error by one lane in the one point – could increase robustness further.



(a) Construction of the values Δy in the clustered points.

$\Delta y_{i-s/2-1,1}$	$\Delta y_{i-s/2,1}$	$\Delta y_{i,1}$	$\Delta y_{i+1,1}$	$\Delta y_{i+s/2,1}$	$\Delta y_{i+s/2+1,1}$
$\Delta y_{i-s/2-1,2}$	$\Delta y_{i-s/2,2}$	$\Delta y_{i,2}$	$\Delta y_{i+1,2}$	$\Delta y_{i+s/2,2}$	$\Delta y_{i+s/2+1,2}$
\vdots	\vdots	\vdots	\vdots	\vdots	\vdots
$\Delta y_{i-s/2-1,n-1}$	$\Delta y_{i-s/2,n-1}$	$\Delta y_{i,n-1}$	$\Delta y_{i+1,n-1}$	$\Delta y_{i+s/2,n-1}$	$\Delta y_{i+s/2+1,n-1}$
$\Delta y_{i-s/2-1,n}$	$\Delta y_{i-s/2,n}$	$\Delta y_{i,n}$	$\Delta y_{i+1,n}$	$\Delta y_{i+s/2,n}$	$\Delta y_{i+s/2+1,n}$
Standard method			Clustered method		

(b) Overview of the values taken for creating the probability distribution function, in which n indicates the number of trajectories and s indicates the number of base points over which the clustering takes place.

Fig. 10. Construction of the values Δy taken for the clustered distribution function

At the beginning of the section, the test vehicle had to drive from the on-ramp onto the main road, and at the end, the test vehicle had to leave the section at an off-ramp. Hence, the trajectories are not well spread over the lanes, and the estimation procedure does not work correctly in this case. It should be noted that this is not a weakness of the methodology, but more of the experimental set-up (one vehicle, always taking the same on-ramp and off-ramp).

VI. INCREASING THE ROBUSTNESS: CLUSTERING

The method can be improved for low numbers of trajectories. To this end, we introduce in this section a method which increases the number of data points in each histogram, and hence improves the robustness of the optimization technique. The mathematical optimization of the method described in this section is the same as in section V-A. The difference is that the points are first clustered such that the optimization can be done with more points (compare the number of observations in figure 9(a) and figure 11(a)). First, the methodology is introduced and in section VI-B results are presented.

A. Methodology

The basic principle for the clustering is that for each point, the lateral offsets (Δy) are calculated as explained in section V-A1. Now, for 10 adjacent points, all values Δy are combined into one distribution function (see figure 10).

The main requirement for this methodology to work is that the lateral positions relative to the respective base points Δy are independent. That holds only if (1) the measurement error is independent, (2) the position of the lanes is the same for all base points included into the clustered point and (3) the lateral position of the lateral offsets for one vehicle at different points combined in a clustered point is not fully correlated. Note that

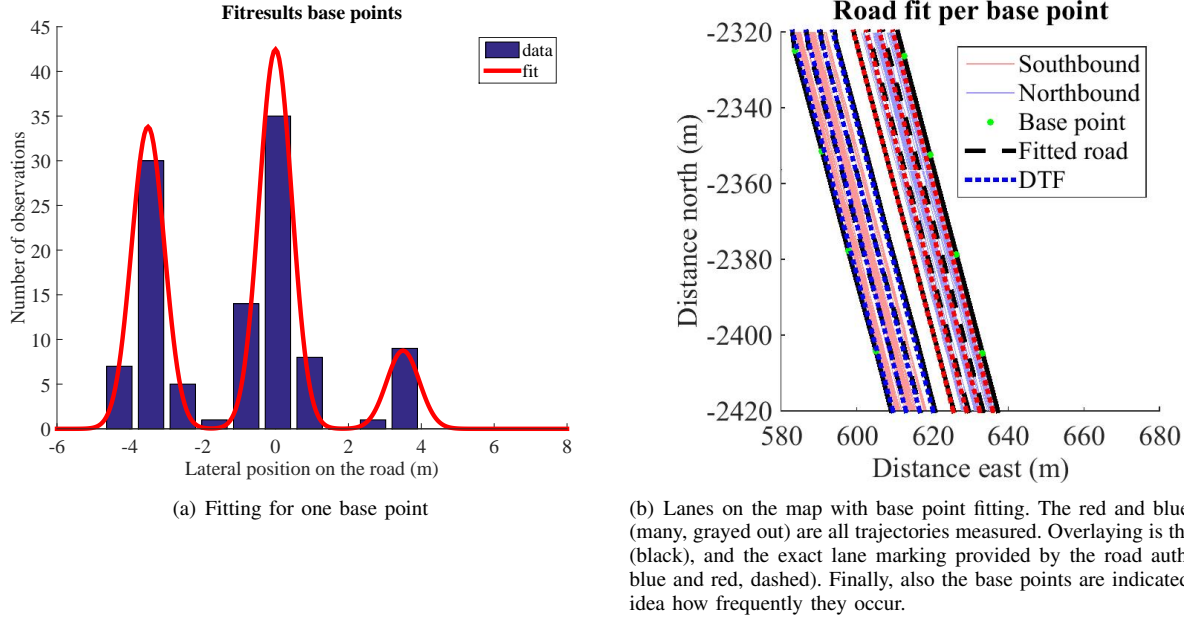


Fig. 9. Results of the lane finding methodology

even if the road itself is curved, requirement 2 is not violated, as long as the base points follow the road profile. With a low number of trajectories at a high sampling rate, requirement 3 is violated (one vehicle chooses one lateral position through the road stretch, so no lanes are visible).

We choose to combine the lateral offsets of ten nodes and assign these to the middle base point, which we will call a *clustered point*; with the chosen distances between the points, this equals approximately 150 m.

B. Results

From the histogram in figure 11(a), it is clear that the lanes can be determined much more robustly. In fact, the lanes can easily be seen in the distribution of the lateral position. The fitting can therefore be done in a much more robust way, leading to a road profile as shown in figure 11(b). Also here, the lanes follow the known locations of lane markings very accurately (error in the order of dm) in the southbound direction. In the northbound direction, the lanes are less accurate, but still good. The quality is good enough so that the trajectory of a vehicle in a lane is indeed mapped onto the lane it is driving in.

This shows that it is possible to create a lane map with just 100 measurements. Using the technique of clustered nodes, the number of measurement points can artificially be further increased for a higher reliability. The requirement that the lateral positions at different base points are not correlated holds reasonably well for 100 trajectories. With a traffic management system implemented in practice one will easily collect many more trajectories than just 100.

VII. CLUSTERED POINTS AND VARIABLE LANE WIDTH

The situation with the clustered base points gives a clear profile for the lateral distribution of passing points. Therefore,

we fit the distribution function without the lane width being known. We do assume all lanes still have the same width. That means for a three lane road, five parameters have to be found: the offset of the first lane, the width of the distribution (σ), the lane width, and for two lanes the fraction of the flow travelling in that lane (the fraction of flow in the third lane can be determined by the fraction of flow in the other two lanes). The difference of the method described in this section compared to section VI is that parameter w in equation (1) is now also estimated in the optimization, rather than taken from the handbook.

The results of this fitting procedure are shown in figure 12(a). The result is similar in quality to when the lane width has been put in exogenously. The optimization procedure does also lead to a quite correct lane width estimation.

Figure 12(b) shows that the procedure works quite well in following the road, with the estimated lane separations in the order of 1 dm off the exact position of the lane markings. The positioning of the southbound lane separations is very accurate and the positioning of the northbound lane separations is less accurate, but still well within the required bounds for practical purposes.

The clustering method requires the same lane layout for all base points which are to be clustered into one clustered point. This means the number of lanes and the lane width should be the same. Although from a theoretical perspective this is a strict requirement, some variations are possible. For instance, small variations in the lane width will not be too problematic, since it can be captured in the intrinsic lateral error of the drivers and the device (σ). Moreover, even if a lane width changes abruptly within the distances covered by one clustered point, drivers will need space to adapt. The trajectories of the vehicles, hence, do not show the same abrupt change of lane width. Therefore, averaging over approximately 150 meters,

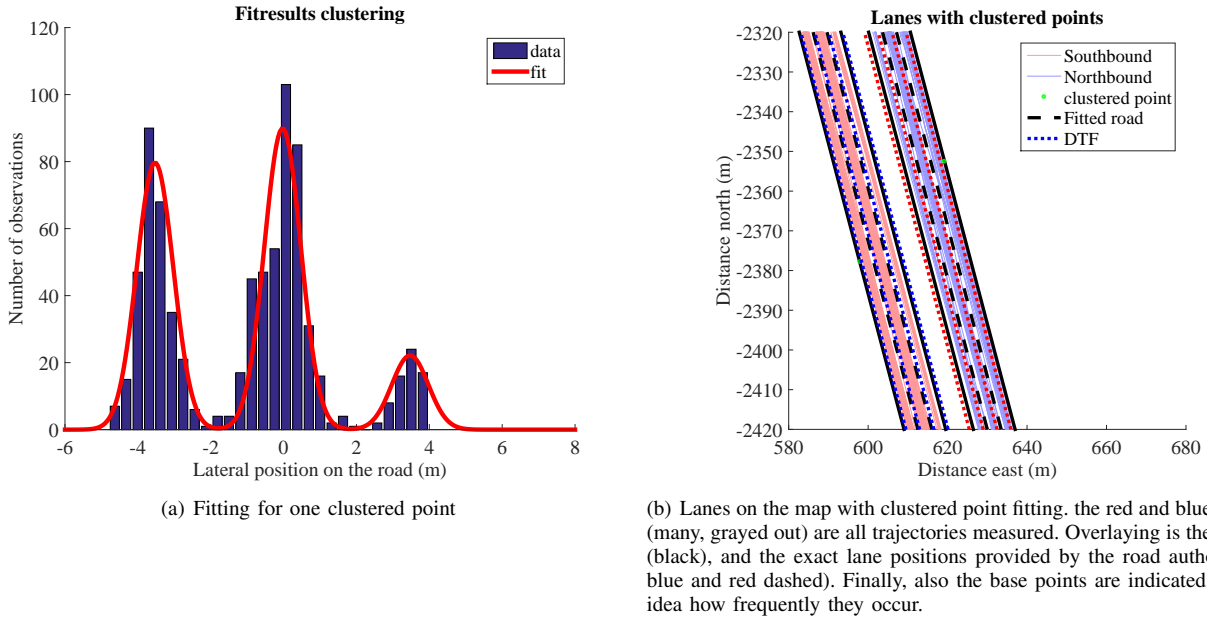


Fig. 11. The results of the fitting process for clustered points

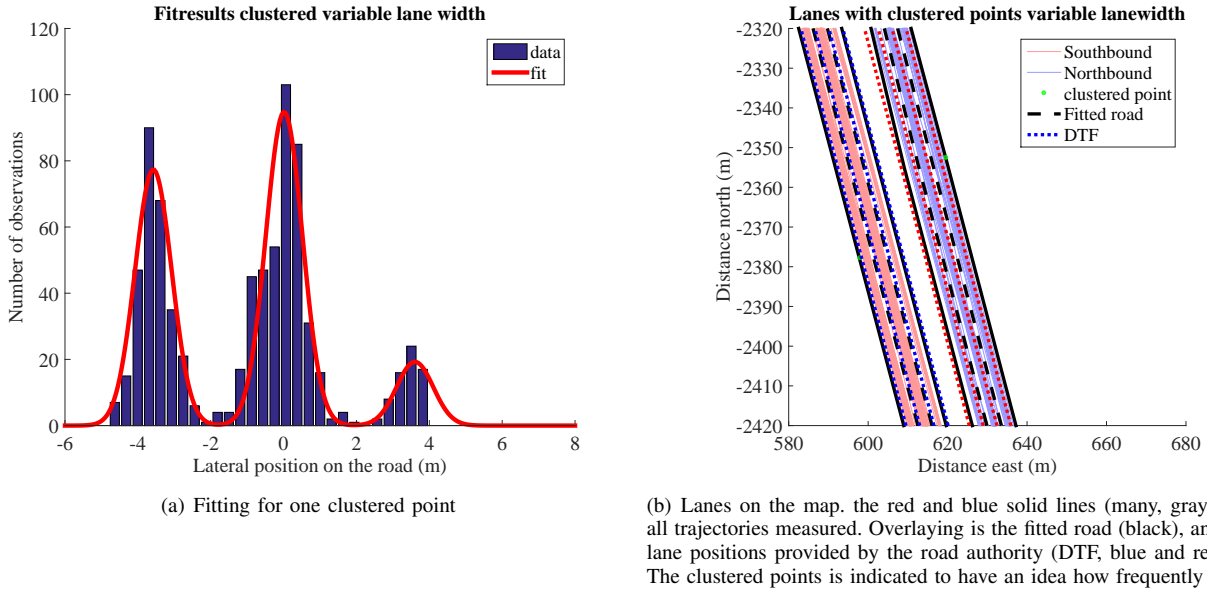


Fig. 12. The results of the fitting process for clustered points and variable lane width

as done here, will most likely also work for stretches with different lane widths to find the lanes, but the positioning of the lane separations will be known less accurately. It depends on the application whether that is accurate enough or not.

The estimated lane width along the northbound road stretch is shown in figure 13. The figure shows the middle part where the distribution of lanes is not influenced by the on and off ramps. In the process shown here, the lane width is estimated every cluster point. If one would know the lanes have the same width, one could also estimate the lane width once for all lanes. For the observations, the median of the estimated lane width is 3.70m – very close to the design width of 3.75m.

VIII. CONCLUSIONS AND OUTLOOK

In this paper, we introduced a GPS single frequency Precise Point Positioning technique. The positions are sufficiently accurate to track a vehicle down to the lane level. To this end, a roadmap with individual lanes is required, which can be collected using the very same GPS single frequency PPP technique; the algorithms to do this have been outlined and demonstrated (in practice) successfully in this paper. The accuracy of lane mapping is very good, once traffic is spread over all lanes.

This technique can be used to get lane-specific traffic information, or to perform lane-specific traffic management. In

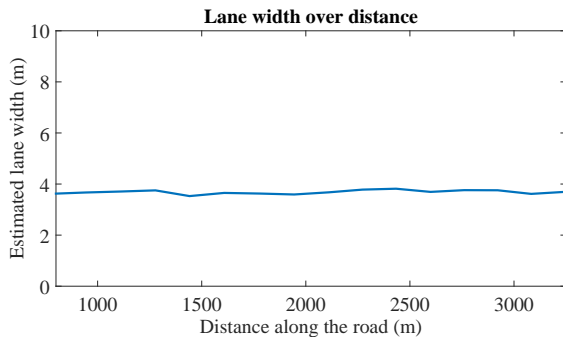


Fig. 13. Estimated lane widths as function of distance (northbound). Again, in the first 500m and after 4000m of distance, the test vehicle does not travel in the designated lanes, but is merging into, or out of the main road, so trajectories are not distributed over the lanes.

order to use the GPS-PPP map, a low bandwidth connection to the vehicles is necessary, in order to provide the system with the position of the satellites, the clock errors and the atmospheric conditions. Moreover, for lane-specific management, it is required that the vehicles communicate their own measured position in real-time (order: tens of seconds) with a central server.

Finally, the current tests showed that the system and the methodology work for flat roads and open surroundings. Some GPS errors are related to receiving the GPS signal without obstruction or reflection. Figure 5 gave a first indication of this, by showing the degraded performance with only 4 GPS satellites available, and to a lesser extent with 5 satellites available. The sensitivity of the GPS-PPP measurements to the different physical environments (hills, urban environments) is topic for further research.

ACKNOWLEDGMENT

The research reported in this paper was conducted as part of the Connected Cruise Control project funded by the Dutch Ministry of Economic Affairs under the High Tech Automotive Systems program, by the universities of Delft, Twente and Eindhoven and NXP, NAVTEQ, TNO, Clifford, Technolution, Rijkswaterstaat and SWOV, as well as the Dutch the Netherlands Organisation for Scientific Research (NWO) in the projects “there is plenty of room in the other lane” and “Taking the Fast Lane” (grant STW-OTP 13771), funded by the STW Technology Foundation of the Netherlands Organisation for Scientific Research

REFERENCES

- [1] A. Chen, A. Ramanandan, J. Farrell, *et al.*, “High-precision lane-level road map building for vehicle navigation,” in *Position Location and Navigation Symposium (PLANS)*, 2010 IEEE/ION. IEEE, 2010, pp. 1035–1042.
- [2] Y.-W. Seo, C. Urmson, and D. Wettergreen, “Ortho-image analysis for producing lane-level highway maps,” in *Proceedings of the 20th International Conference on Advances in Geographic Information Systems*, 2012.
- [3] A. Joshi and M. R. James, “Generation of accurate lane-level maps from coarse prior maps and lidar,” *Intelligent Transportation Systems Magazine, IEEE*, vol. 7, no. 1, pp. 19–29, 2015.
- [4] R. J. P. Van Bree, P. J. Buist, C. C. J. M. Tiberius, B. Van Arem, and V. L. Knoop, “Lane identification with real time single frequency precise point positioning: A kinematic trial,” in *Proceedings of Institute of Navigation’s Satellite Division Technical Meeting (ION GNSS)*, Portland, Oregon, 21–23 September 2011, pp. 314–323.
- [5] V. L. Knoop, C. C. J. M. Tiberius, P. J. Buist, and B. van Arem, “Precise Point Positioning: affordable GPS positioning accurate to lane-level,” in *Proceedings of the IEEE conference on Intelligent Transport Solutions*, 16–19 September 2012 2012.
- [6] V. L. Knoop, P. de Bakker, C. Tiberius, and B. van Arem, “Single frequency precise point positioning: obtaining a map accurate to lane-level,” in *Intelligent Transportation Systems-(ITSC), 2013 16th International IEEE Conference on*. IEEE, 2013, pp. 2255–2261.
- [7] I. Skog and P. Händel, “In-car positioning and navigation technologies – a survey,” *Intelligent Transportation Systems, IEEE Transactions on*, vol. 10, no. 1, pp. 4–21, 2009.
- [8] X. Zhao, “On processing GPS tracking data of spatio-temporal car movements: a case study,” *Journal of Location Based Services*, pp. 1–19, 2015.
- [9] C. Fouque and P. Bonnifait, “Matching raw GPS measurements on a navigable map without computing a global position,” *Intelligent Transportation Systems, IEEE Transactions on*, vol. 13, no. 2, pp. 887–898, 2012.
- [10] Y. Cui and S. S. Ge, “Autonomous vehicle positioning with GPS in urban canyon environments,” *Robotics and Automation, IEEE Transactions on*, vol. 19, no. 1, pp. 15–25, 2003.
- [11] J. Farrell and T. Givargis, “Differential GPS reference station algorithm-design and analysis,” *Control Systems Technology, IEEE Transactions on*, vol. 8, no. 3, pp. 519–531, 2000.
- [12] J. Du and M. Barth, “Bayesian probabilistic vehicle lane matching for link-level in-vehicle navigation,” in *Intelligent Vehicles Symposium, 2006 IEEE*. IEEE, 2006, pp. 522–527.
- [13] W. Wang, H. Chen, and M. C. Bell, “Vehicle Breakdown Duration Modeling,” *Journal of Transportation and Statistics*, vol. 8, no. 1, pp. 75–84, 2005.
- [14] M. A. Sotelo, F. J. Rodriguez, and L. Magdalena, “Virtuous: Vision-based road transportation for unmanned operation on urban-like scenarios,” *Intelligent Transportation Systems, IEEE Transactions on*, vol. 5, no. 2, pp. 69–83, 2004.
- [15] Z. Tao and P. Bonnifait, “Road invariant extended kalman filter for an enhanced estimation of GPS errors using lane markings,” in *Intelligent Robots and Systems (IROS), 2015 IEEE/RSJ International Conference on*. IEEE, 2015, pp. 3119–3124.
- [16] A. B. Hillel, R. Lerner, D. Levi, and G. Raz, “Recent progress in road and lane detection: a survey,” *Machine Vision and Applications*, vol. 25, no. 3, pp. 727–745, 2014.
- [17] Y. U. Yim and S.-Y. Oh, “Three-feature based automatic lane detection algorithm (TFALDA) for autonomous driving,” *Intelligent Transportation Systems, IEEE Transactions on*, vol. 4, no. 4, pp. 219–225, 2003.
- [18] J. C. McCall and M. M. Trivedi, “Video-based lane estimation and tracking for driver assistance: survey, system, and evaluation,” *Intelligent Transportation Systems, IEEE Transactions on*, vol. 7, no. 1, pp. 20–37, 2006.
- [19] Z. Kim, “Robust lane detection and tracking in challenging scenarios,” *Intelligent Transportation Systems, IEEE Transactions on*, vol. 9, no. 1, pp. 16–26, 2008.
- [20] Q. Li, N. Zheng, and H. Cheng, “Springrobot: A prototype autonomous vehicle and its algorithms for lane detection,” *Intelligent Transportation Systems, IEEE Transactions on*, vol. 5, no. 4, pp. 300–308, 2004.
- [21] J. Wang, S. Schroedl, K. Mezger, R. Ortloff, A. Joos, and T. Passegger, “Lane keeping based on location technology,” *Intelligent Transportation Systems, IEEE Transactions on*, vol. 6, no. 3, pp. 351–356, 2005.
- [22] R. Toledo-Moreo, D. Bétaille, and F. Peyret, “Lane-level integrity provision for navigation and map matching with GNSS, dead reckoning, and enhanced maps,” *Intelligent Transportation Systems, IEEE Transactions on*, vol. 11, no. 1, pp. 100–112, 2010.
- [23] V. Milanés, J. E. Naranjo, C. González, J. Alonso, and T. de Pedro, “Autonomous vehicle based in cooperative GPS and inertial systems,” *Robotica*, vol. 26, no. 05, pp. 627–633, 2008.
- [24] J. F. Zumberge, M. B. Hefflin, D. C. Jefferson, M. M. Watkins, and F. H. Webb, “Precise point positioning for the efficient and robust analysis of GPS data from large networks,” *JOURNAL OF GEOPHYSICAL RESEARCH*, vol. 102, pp. 5005–5017, 1997.
- [25] S. Bisnath and Y. Gao, “Current state of precise point positioning and future prospects and limitations,” in *Observing our changing earth*. Springer, 2009, pp. 615–623.

- [26] R. van Bree, C. Tiberius, and A. Hauschild, "Real time satellite clocks in single frequency precise point positioning," in *Proceedings of Institute of Navigation's Satellite Division Technical Meeting (ION GNSS)*, Savannah, Georgia, USA, September 22-25 2009, pp. 2400–2414.
- [27] S. Loyer, F. Perosanz, F. Mercier, H. Capdeville, and J.-C. Marty, "Zero-difference GPS ambiguity resolution at CNES–CLS IGS analysis center," *Journal of Geodesy*, vol. 86, no. 11, pp. 991–1003, 2012.
- [28] T. Yunck, *Global positioning systems: Theory and applications. Progress in Astronautics and Aeronautics, Volume 163*. American Institute of Aeronautics and Astronautics, Inc., 1996, ch. Orbit Determination. In (Eds.).
- [29] Y. Chen, J. Liu, L. Ruotsalainen, L. Chen, T. Kröger, H. Kuusniemi, L. Pei, R. Chen, T. Tenhunen, and Y. Wang, "Lane detection based on a visual-aided multiple sensors platform," in *Position Location and Navigation Symposium (PLANS), 2012 IEEE/ION*. IEEE, 2012, pp. 740–747.
- [30] R. van Bree and C. Tiberius, "Real-time single-frequency precise point positioning: accuracy assessment," in *GPS Solutions*, vol. 16. Springer-Verlag, 2012, pp. 259–266.
- [31] J. Dow, R. Neilan, and G. Gendt, "The International GPS Service (IGS): Celebrating the 10th Anniversary and Looking to the Next Decade." *Advances in Space Research*, vol. 36, no. 3, pp. 320–326, 2005.
- [32] S. Schaer, G. Beutler, and M. Rothacher, "Mapping and predicting the ionosphere," in *Proceedings of the IGS Analysis Center Workshop*, J. M. Dow, J. Kouba, and T. Springer, Eds., February 9-11 1998, pp. 307–318.
- [33] J. Saastamoinen, "Atmospheric correction for the troposphere and stratosphere in radio ranging of satellites, the use of artificial satellites for geodesy," *Geophysics Monograph Series*, vol. 15, pp. 247–251, 1972.
- [34] www.kadaster.nl/rijksdriehoeksmeting/netpos/, in Dutch.
- [35] E. Kaplan and C. J. Hegarty, Eds., *Understanding GPS: principles and applications*, 2nd ed. ARTECH HOUSE, INC. Norwood, MA, USA, 2006.
- [36] P. Misra and P. Enge, Eds., *Global Positioning System - Signals, Measurements, and Performance*, 2nd ed. Ganga-Jamuna Press, USA, 2010.

Victor L. Knoop received his Master's degree in Physics from Leiden University (2005), and his PhD degree from Delft University of Technology (2009) on the effects of incidents on driving behaviour and traffic congestion. After a post-doc at the university of Lyon (2009-2010) on lane changing, Victor Knoop now holds a tenured assistant professorship at the Delft University of Technology. His main research interest is the interaction between microscopic and macroscopic traffic flow phenomena.

Peter de Bakker Peter de Bakker obtained his MSc-degree in Aerospace Engineering at Delft University of Technology in the Netherlands and has recently completed his PhD-research on Precise Point Positioning and Integrity Monitoring.

Christian Tiberius Christian Tiberius is an associate professor at Delft University of Technology. He has been involved in GNSS positioning and navigation research since 1991, currently with emphasis on data quality control, satellite-based augmentation systems, and precise point positioning.

Bart van Arem holds a Master's degree (1986) and PhD degree (1990) in Applied Mathematics, speciality queueing theory at the University of Twente, the Netherlands. He has worked as a researcher and program manager at TNO between 1992 and 2009 on Intelligent Transport Systems, in which he has been active in various national and international projects. His interest focuses on Advanced Driver Assistance systems. Since 2009 he is a full professor Transport & Planning at Delft University of Technology, focusing on the impact of Intelligent Transport Systems on mobility.